

Nanoemulsions Induced by Compressed Gases**

Jianling Zhang, Buxing Han,* Chaoxing Zhang, Wei Li, and Xiaoying Feng

An emulsion is a heterogeneous system consisting of at least two immiscible liquids. Emulsions have been an important research topic for years, and they are widely used in cleaning, material science, chemical reactions, manufacturing, enhanced oil recovery, and many other processes.^[1–7] Emulsions with submicrometer droplet size—so-called nanoemulsions—have attracted much attention in recent years.^[8,9] As a result of their small droplet size, such nanoemulsions may appear transparent or translucent. Furthermore, they present unusual properties relative to the macro- or microemulsions; for example, the droplets in nanoemulsions are better dispersed than those in macroemulsions, and they also possess a higher stability against sedimentation, creaming, flocculation, and coalescence. In contrast to microemulsions, a lower surfactant concentration is required for the formation of nanoemulsions, and the volume fraction of the dispersed component can be much larger. Several techniques for preparing nanoemulsions have been reported; these include applying mechanical energy,^[10] changing the temperature,^[11] or using additives.^[12,13] It is known that the use of additives, such as co-surfactants or salts, may lead to higher material costs as well as to the contamination or modification of the products by these additives. The development of effective, controllable, and environmentally benign methods to prepare nanoemulsions is challenging and of great importance.

Compressed gases (for example, CO₂) are very soluble in many organic solvents, their solubility depending on the temperature and the pressure. Dissolution of gases in liquids can change the properties of the liquid solvents considerably. Therefore, the properties of liquid solvents can be tuned continuously by controlling the pressure of the gases.^[14] This principle has been applied to different processes, such as tuning the properties of chemical reactions,^[15,16] controlling the stability of reverse micelles,^[17] material processing,^[18–20] polymerization promotion,^[21] and as to change the characteristics of the mobile phase in HPLC.^[22] The applications of gas-expanded liquids have been recently reviewed.^[23]

Here, we demonstrate—for the first time—that compressed gases, such as CO₂, ethylene, ethane, and propane, can induce the formation of a number of nanoemulsions with the following special advantages: 1) the surfactant concentration

can be very low; 2) the nanoemulsions can be formed in a wide range of water-to-oil volume ratios; 3) formation and breakage of the nanoemulsions are reversible and can be controlled by pressurization and depressurization; 4) the gas can be easily removed by reducing the pressure; 5) the method is environmentally benign. Furthermore, conventional additives are usually strongly polar (or ionic) liquids or solids whereas in our method nonpolar gases are used. The mechanism of the formation of nanoemulsions using nonpolar gases can be very different from that observed with conventional additives. Therefore, this study may trigger further work on several interesting fundamental and practical topics. As examples, we investigated the applications of CO₂-induced nanoemulsions in the preparation of cross-linked porous polystyrene materials as well as the ability of CO₂ to stabilize emulsions in enhanced oil recovery. We achieved promising results in both cases. A possible mechanism for the formation of this kind of nanoemulsions is also discussed.

The water/sodium bis-2-ethylhexylsulfosuccinate (AOT)/isooctane system (with a surfactant concentration of 0.02 g mL⁻¹ and equal volumes of water and isooctane) becomes completely turbid upon stirring, which agrees with the water/AOT/isooctane ternary phase diagram reported in the literature.^[24] Interestingly, we found that the turbid emulsion became more transparent as CO₂ was added to the system under stirring, and a complete transparent emulsion was obtained when the CO₂ pressure reached 3.78 MPa at 303.2 K. Subsequently, with continuously increasing CO₂ pressure, the transparent emulsion changed into turbid again. This change can be clearly observed in Figure 1a–g. Here, we define the pressure at which the emulsion becomes completely transparent as the “transpar-

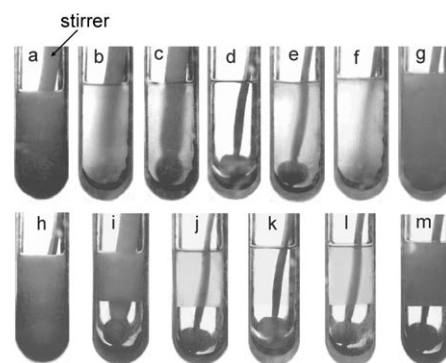


Figure 1. Photographs of the H₂O/AOT/isooctane system at 303.2 K and CO₂ pressures of: a) 0 MPa, b) 3.55 MPa, c) 3.64 MPa, d) 3.78 MPa, e) 3.90 MPa, f) 4.01 MPa, and g) 4.45 MPa; h) corresponds to (d) after releasing of CO₂; i–m) correspond to (a), (c), (d), (e), and (g), respectively, after phase separation for 72 h; [AOT] = 0.02 g mL⁻¹, water/oil (1:1, v/v).

[*] Dr. J. Zhang, Prof. B. Han, C. Zhang, W. Li, X. Feng
Beijing National Laboratory
for Molecular Sciences, Institute of Chemistry
Chinese Academy of Sciences, Beijing (China)
Fax: (+) 86-10-6255-9373
E-mail: hanbx@iccas.ac.cn

[**] The authors acknowledge the National Natural Science Foundation of China for financial support (20633080, 20403021).

Supporting information for this article is available on the WWW under <http://www.angewandte.org> or from the author.

ency pressure" P_T . The transparency of the emulsion at P_T is indicative of much a smaller droplet size relative to the turbid emulsions at lower or higher pressures. In addition, the formation of the nanoemulsion was reversible and could be repeated by controlling the pressure. After releasing CO_2 , the nanoemulsion shown in Figure 1d changed into a turbid emulsion, as shown in Figure 1h. However, the transparent nanoemulsion (Figure 1d) could be recovered by compressing the gas again to 3.78 MPa.

It is known that both micro- and nanoemulsions are transparent. Sedimentation analysis is often used to differentiate between them because a microemulsion is thermodynamically stable whereas a nanoemulsion is not. We studied the stability of the emulsions at different conditions. Our experiments demonstrated that the transparent emulsion shown in Figure 1d was not thermodynamically stable. The emulsion separated into water-rich and isooctane-rich phases after stirring had been stopped for a certain time. Therefore, we conclude that the transparent emulsion shown in Figure 1d is a nanoemulsion. The photographs of the emulsions at different pressures after phase separation are shown in Figure 1i–m.

The stability of emulsions can be evaluated qualitatively by determining the phase-separation rate or the dependence of the volume of the aqueous phase on time after stopping the stirrer. We found that the increase in the volume of water—caused by dissolution of CO_2 —was negligible under our experimental conditions. Therefore, the stability of the emulsions at different pressures can be characterized by the variation in the ratio between the aqueous phase and the total volume of water and isooctane with time. The results, obtained at different CO_2 pressures, are shown in Figure 2. In the absence of CO_2 , the $\text{H}_2\text{O}/\text{AOT}/\text{isooctane}$ system was very unstable, and the aqueous phase appeared within one minute after stopping the stirrer; complete phase separation occurred after about 7 h. However, by adding CO_2 , the time for complete phase separation could be significantly prolonged. At a pressure of 3.78 MPa, the aqueous phase appeared after the stirrer had been stopped for about 15 min and it took about 60 h for complete phase separation to occur. At higher CO_2 pressures, the emulsion was turbid but still very stable.

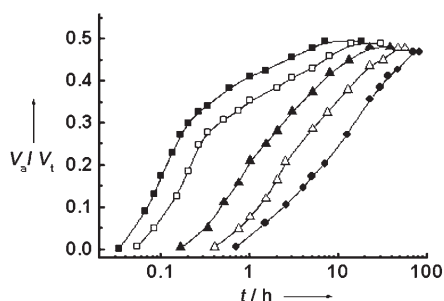


Figure 2. Dependence of the ratio of the separated aqueous phase and the total liquid mixture (V_a/V_t) on time for the system $\text{H}_2\text{O}/\text{AOT}/\text{isooctane}$ at 303.2 K and CO_2 pressures of 0 MPa (■), 2.15 MPa (□), 3.64 MPa (▲), 3.78 MPa (△), and 4.72 MPa (●); $[\text{AOT}] = 0.02 \text{ g mL}^{-1}$, water/oil (1:1, v/v).

We studied the emulsion cross-linking polymerization of styrene at 313.2 K in the emulsion system water/AOT/styrene/toluene/diethylenebenzene (where diethylenebenzene acts as the cross-linker). The ratio of water/styrene/toluene/diethylenebenzene was 2.6:1.5:1:0.08 (v/v) and the concentration of AOT was 0.02 g mL^{-1} . The P_T of the system determined at this temperature was 6.80 MPa. Turbid emulsions were formed at lower or higher pressures. Transmission electron microscopy (TEM) images of the cross-linked polystyrene products obtained from the emulsions at different pressures are shown in Figure 3. In the absence of CO_2 and at pressures

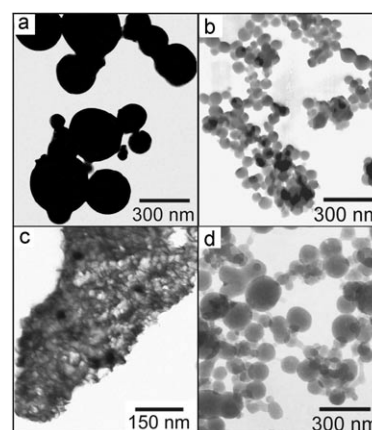


Figure 3. TEM images of cross-linked polystyrene obtained at 313.2 K and a) 0 MPa, b) 4.16 MPa, c) 6.80 MPa, and d) 7.45 MPa; $[\text{AOT}] = 0.02 \text{ g mL}^{-1}$, water/monomer phase (1:1, v/v).

of 4.16 and 7.45 MPa (at which turbid macroemulsions were formed with larger droplets), the cross-linked polymer particles exhibited sizes and shapes that were typical for polymerization products in conventional macroemulsions (Figure 3a,b,d). Interestingly, in the nanoemulsion at 6.80 MPa, a porous polymeric material with an average pore size of about 20 nm was obtained (Figure 3c). Emulsion polymerization has been widely studied (including the emulsion cross-linking polymerization of styrene). In macroemulsion polymerization, microparticles are generated via the capture of free radicals by micelles, which exhibit an extremely large oil/water interfacial area. In general, monomer droplets are not effective in competing with micelles to capture the free radicals generated in the aqueous phase, because of their relatively small surface area, and they mainly serve as reservoirs to supply the growing particles with monomer and surfactant species;^[25] therefore, spherical particles are usually produced. Nanoemulsion polymerizations show quite different particle nucleation and growth mechanisms than those of conventional macroemulsion polymerizations.^[26,27] The monomers are mainly polymerized in situ because of the much larger monomer/water interfacial area, and therefore, the morphology of the cross-linked polymers reflects the microstructure of the nanoemulsions. In this case, we can deduce from the porous structure of the cross-linked polystyrene that the oil formed a continuous phase, in which nanoscaled water droplets were dispersed.

Both compressed CO₂ and surfactants have been widely used in enhanced oil recovery.^[6,28,29] Compressed CO₂ can expand the oils, reduce their viscosity, and provide a driving force for oil recovery. Surfactants, on the other hand, can reduce the water/oil interfacial tension to emulsify the mixture. An efficient emulsification can then increase the recovery rate. We also studied the effect of CO₂ on the stability of the water/AOT/crude oil emulsion system. The concentration of AOT was 0.02 g mL⁻¹ and the crude-oil-to-water ratio was 1:1 (v/v). The results are demonstrated in Figure 4. An obvious phase separation could be observed

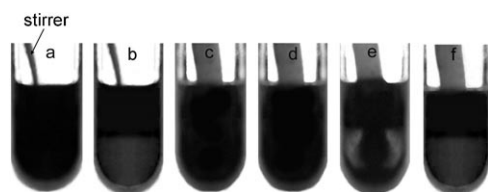


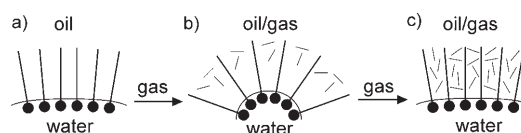
Figure 4. Photographs of the H₂O/AOT/crude oil system at 303.2 K in the absence of CO₂ [with stirring (a) and 30 min after stopping the stirrer (b)] and in the presence of CO₂ [$P = 6.61$ MPa, with stirring (c) and 24 h (d) and 48 h (e) after stopping the stirrer]; f) corresponds to photograph (c) after releasing of CO₂ for 30 min; [AOT] = 0.02 g mL⁻¹, water/oil (1:1, v/v).

30 min after stopping the stirrer in the absence of CO₂ (Figure 4b). However, CO₂ could stabilize the emulsion efficiently. At a pressure of 6.61 MPa, no evidence of separation was observed up to 24 h after turning off the stirrer (Figure 4d). Evident phase separation was observed after 48 h (Figure 4e). The reversibility and repeatability of the stabilization process in this emulsion was also tested. For the emulsion at 6.61 MPa, separation could be observed after releasing CO₂ for 30 min (Figure 4f). This result is interesting for the petroleum industry because CO₂ can enhance emulsification, thus providing a driving force for oil recovery, and after the oils have been recovered, the emulsions can be demulsified quickly by releasing CO₂ at ambient pressure.

We also studied the effect of the concentration of AOT, the temperature, the water-to-oil volume ratio, and the number of carbon atoms in the oil (*n*-alkanes) on the value of P_T . The microstructure of the nanoemulsions was further characterized by means of conductivity measurement and UV/Vis spectroscopy. Besides the described system, which contains the anionic surfactant AOT, we also studied the formation of compressed-gas-induced nanoemulsions in systems containing other two surfactants, namely, cetyltrimethylammonium bromide (CTAB, a typical cationic surfactant) and TritonX-100 (a commonly used nonionic surfactant). Nanoemulsion formation induced by other gases, namely, ethylene, ethane, and propane was also investigated. We found that P_T decreased with increasing surfactant concentration and decreasing temperature, and that the nanoemulsions could be formed in a wide range of water-to-isooctane volume ratios. Also, the value of P_T was observed to increase with increasing number of carbon atoms in the *n*-alkanes, which acted as oils. The cationic and nonionic surfactants

could also form gas-induced nanoemulsions, and all the gases tested herein were found to induce the formation of nanoemulsions. The value of P_T was found to be lower in those systems exhibiting a better compatibility between the gas and the surfactant chains. The polarity of the water droplets in the nanoemulsions was similar to that of the bulk water. Furthermore, the size of the droplets in the nanoemulsions was the smallest, which is consistent with the direct observation shown in Figure 1. Detailed results and discussions to the experiments described in this paragraph are presented in the Supporting Information.

The results presented above indicate that the gas-induced formation of nanoemulsions is a general phenomenon. At present, it is still challenging to provide an exact mechanism for this interesting behavior (although it is of great importance from both theoretical and practical points of views). Further studies are thus required. One of the main reasons for this phenomenon could be that the gas molecules can insert into the water/oil interfacial films formed by the surfactants because of their smaller sizes (relative to those of the oils). The insertion of the gas molecules may increase the natural curvature (reducing radius) of the dispersed droplets, if the gases in the films exist mainly in the shallow region (Scheme 1b). Therefore, the size of the droplets is reduced and nanoemulsions can be formed at a suitable pressure. However, if an excess of gas is added, the gas molecules can also penetrate into deeper regions of the interfacial films, thus making the hydrocarbon tails of the surfactants become more parallel again; therefore, the curvature of the droplets decreases with the pressure, that is, the size of the droplets increases with the pressure (see Scheme 1c). The insertion of gases into the interfacial films also increases the rigidity of those films, which is favorable for enhancing the stability of the emulsions. Therefore, the emulsions can also be stabilized by gases at higher pressures, although in those cases, the droplet sizes are larger than those of nanoemulsions. This argument not only explains how the size of the emulsions changes with the pressure, but it can also clarify other experimental results obtained in this work, for example: 1) The value of P_T increases with increasing number of carbon atoms in the oils (*n*-alkanes). It is more difficult for an alkane with a longer chain to penetrate into the interfacial films effectively.^[30] Thus, more gas is needed to insert it and form the nanoemulsions; 2) The gases can induce the formation of nanoemulsions, although our experiments showed that *n*-pentane does not exhibit this property because of its larger size; 3) A gas exhibiting a good compatibility with the surfactant chains has a lower P_T value, because it is easier to insert it into the interfacial region. Detailed discussions are presented in the Supporting Information.



Scheme 1. Induction of nanoemulsions and stabilization of emulsions by insertion of gases (—) into the interfacial region of the emulsions.

In summary, we have shown that compressed gases, such as CO₂, ethylene, ethane, and propane, can induce the formation of nanoemulsions with special characteristics. We believe that this new type of nanoemulsions will extend the scope of fundamental research and applications in this area. Future work will include additional studies on the mechanisms involved as well as an evaluation of the possible applications of gas-induced nanoemulsions and gas-stabilized emulsions in different fields like materials science, chemical reactions, and the pharmaceutical and oil industries.

Experimental Section

The apparatus used for the phase-behavior investigations was similar to that employed previously for studying reverse micelle solutions at elevated pressures.^[17] It consisted of a view cell with stirrer, a high-pressure pump, a constant-temperature water bath, and a pressure gauge. In a typical experiment, the desired amount of surfactant, water, and oil were added into the view cell and the mixture was stirred. After thermal equilibrium was reached, the gas was charged into the view cell to the desired pressure, and the phase behavior was observed.

The apparatus described above was also used to study the polymerization process. In the experiment, a known amount of AOT was dissolved in a mixture of styrene/toluene/DVB (1.5:1:0.08 v/v/v). Then, water was added to the organic solution (upon stirring) until the volume of both phases was equal. The concentration of AOT was 0.02 g mL⁻¹. After stirring for 30 min, the initiator potassium peroxydisulfate was added to the emulsion upon stirring ([K₂S₂O₈] = 0.9 mg mL⁻¹). The autoclave containing the emulsion was then transferred into a water bath at 313.2 K. Then, CO₂ was charged into the autoclave to the desired pressure (upon stirring). Finally, after a reaction time of 24 h, the gas was released. The separated product was characterized by TEM with a TECNAI 20 PHILIPS electron microscope.

The chemicals and equipment used, as well as the procedures for the UV/Vis and conductivity measurements, are given in the Supporting Information.

Received: November 22, 2007

Revised: December 29, 2007

Published online: March 10, 2008

Keywords: compressed gases · nanoemulsions · polymerization · reaction mechanisms · surfactants

- [2] A. S. Utada, E. Lorenceau, D. R. Link, P. D. Kaplan, H. A. Stone, D. A. Weitz, *Science* **2005**, 308, 537.
- [3] A. D. Dinsmore, M. F. Hsu, M. G. Nikolaides, M. Marquez, A. R. Bausch, D. A. Weitz, *Science* **2002**, 298, 1006.
- [4] K. P. Johnston, K. L. Harrison, M. J. Clarke, S. M. Howdle, M. P. Heitz, F. V. Bright, C. Carlier, T. W. Randolph, *Science* **1996**, 271, 624.
- [5] E. J. Beckman, *Science* **1996**, 271, 613.
- [6] Y. Liu, P. G. Jessop, M. Cunningham, C. A. Eckert, C. L. Liotta, *Science* **2006**, 313, 958.
- [7] J. Eastoe, S. Gold, S. E. Regers, A. Paul, T. Welton, R. K. Heenan, I. Grillo, *J. Am. Chem. Soc.* **2005**, 127, 7302.
- [8] T. Tadros, P. Izquierdo, J. Esquena, C. Solans, *Adv. Colloid Interface Sci.* **2004**, 108–109, 303.
- [9] C. Solans, P. Izquierdo, J. Nolla, N. Azemar, M. J. Garcia-Celma, *Curr. Opin. Colloid Interface Sci.* **2005**, 10, 102.
- [10] P. Walstra in *Emulsion Stability* (Ed.: P. Becher), *Encyclopedia of Emulsion Technology*, Dekker, New York, **1996**, pp. 1–62.
- [11] D. Morales, C. Solans, J. M. Gutiérrez, M. J. Garcia-Celma, U. Olsson, *Langmuir* **2006**, 22, 3014.
- [12] S. Sajjadi, *Langmuir* **2006**, 22, 5597.
- [13] I. Solé, A. Maestro, C. González, C. Solans, J. M. Gutiérrez, *Langmuir* **2006**, 22, 8326.
- [14] C. A. Eckert, B. L. Knutson, P. G. Debenedetti, *Nature* **1996**, 383, 313.
- [15] M. Wei, G. T. Musie, D. H. Busch, B. Subramaniam, *J. Am. Chem. Soc.* **2002**, 124, 2513.
- [16] M. Solinas, A. Pfaltz, P. G. Cozzi, W. Leitner, *J. Am. Chem. Soc.* **2004**, 126, 16142.
- [17] X. Y. Feng, J. L. Zhang, J. Chen, B. X. Han, D. Shen, *Chem. Eur. J.* **2006**, 12, 2087.
- [18] C. N. Field, P. A. Hamley, J. M. Webster, D. H. Gregory, J. J. Titman, M. Poliakoff, *J. Am. Chem. Soc.* **2000**, 122, 2480.
- [19] C. A. Johnson, S. Sharma, B. Subramaniam, A. S. Borovik, *J. Am. Chem. Soc.* **2005**, 127, 9698.
- [20] M. Anand, L. A. Odom, C. B. Roberts, *Langmuir* **2007**, 23, 7338.
- [21] J. Liu, B. X. Han, Z. M. Liu, J. Q. Wang, Q. Huo, *J. Supercrit. Fluids* **2001**, 20, 171.
- [22] H. M. Yuan, S. V. Olesik, *Anal. Chem.* **1998**, 70, 1595.
- [23] P. G. Jessop, B. Subramaniam, *Chem. Rev.* **2007**, 107, 2666.
- [24] B. Tamamushi, N. Watanabe, *Colloid Polym. Sci.* **1980**, 258, 174.
- [25] C. S. Chern, *Prog. Polym. Sci.* **2006**, 31, 443.
- [26] F. J. Schork, Y. W. Luo, W. Smulders, J. P. Russum, A. Butte, K. Fontenot, *Adv. Polym. Sci.* **2005**, 175, 129.
- [27] J. M. Asua, *Prog. Polym. Sci.* **2002**, 27, 1283.
- [28] F. M. Orr, Jr., J. J. Taber, *Science* **1984**, 224, 563.
- [29] J. G. Speight, *The Chemistry and Technology of Petroleum*, 3rd ed., Dekker, New York, **1998**.
- [30] G. J. Mcfann, K. P. Johnson, *J. Phys. Chem.* **1991**, 95, 4889.

[1] T. F. Tadros, *Applied Surfactant—Principle and Applications*, Wiley-VCH, Weinheim, **2005**.